JOURNAL OF CHEMICAL INFORMATION AND MODELING

Article

pubs.acs.org/jcim

Validation of the AmpC β-Lactamase Binding Site and Identification of Inhibitors with Novel Scaffolds

Fung-Yi Chan,[†] Marco A. C. Neves,[‡,§] Ning Sun,[†] Man-Wah Tsang,[†] Yun-Chung Leung,[†] Tak-Hang Chan,[†] Ruben Abagyan,*[,‡] and Kwok-Yin Wong*[,†]

[†]Department of Applied Biology and Chemical Technology and State Key Laboratory of Chirosciences, The Hong Kong Polytechnic University, Hung Hom, Kowloon, Hong Kong, P. R. China

[‡]Skaggs School of Pharmacy & Pharmaceutical Sciences, University of California, San Diego, 9500 Gilman Drive, La Jolla, California 92093, United States

[§]Centro de Neurociências, Lab. Química Farmacêutica, Faculdade de Farmácia, Universidade de Coimbra, Pólo das Ciências da Saúde, 3000-548 Coimbra, Portugal

Supporting Information

ABSTRACT: AmpC β-lactamase confers resistance to β-lactam antibiotics in multiple Gram-negative bacteria. Therefore, identification of non-β-lactam compounds that inhibit the enzyme is considered crucial to the development of novel antibacterial therapies. Given the highly solvent-exposed active site, it is important to study the induced-fit movements and water-mediated interactions to improve docking accuracy and virtual screening enrichments in structure-based design of new AmpC inhibitors. Here, we tested multiple models of the AmpC binding site to investigate the importance of conserved water molecules and binding site plasticity on molecular docking. The results indicate that at least one conserved water molecule greatly improves the binding pose predictions and virtual screening enrichments of known noncovalent AmpC inhibitors. The best model was tested prospectively in the virtual screening of about 6 million commercially available compounds. Sixty-one chemically diverse top-scoring compounds were experimentally tested, which led to the identification of seven previously unknown inhibitors. These findings validate the essential features of the AmpC binding site for molecular recognition and are useful for further optimization of identified inhibitors.

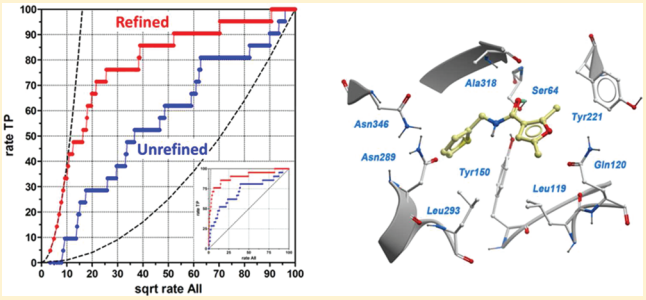

INTRODUCTION

Antibiotic resistance is a serious threat to public health and is responsible for the increase in morbidity, mortality, and health care costs related to the treatment of bacterial infections.[1] Some pathogenic bacteria are not susceptible to widely prescribed β-lactam antibiotics such as penicillins and cephalosporins.[2] Emergence of antibiotic-resistant bacteria is primarily driven by overuse of β-lactam antibiotics in food and agricultural products.[3] Bacterial resistance to β-lactam antibiotics results from multiple mechanisms such as mutation of the molecular targets (penicillin-binding proteins), modification of outer membrane proteins, and active efflux of antibiotics.[4−6] However, the most prominent resistance mechanism is related to the expression of β-lactamase enzymes.[7] β-Lactamases catalyze the hydrolysis of the four-membered cyclic amide ring of β-lactam antibiotics (Chart 1A), thus impairing their ability to interact with penicillin-binding proteins and inhibit bacterial cell wall formation.[8] Class C β-lactamases, such as AmpC, are among the most clinically relevant enzymes.[9,10] AmpC β-lactamases are present in opportunist Gram-negative pathogens such as *Enterobacter* spp. and *P. aeruginosa*.[11] They have a broad spectrum activity to hydrolyze β-lactamase-resistant antibiotics, such as the fifth generation cephalosporins, and can also evade β-lactam-based β-lactamase inhibitors such as clavulanic acid, sulbactam, and tazobactam (Chart 1B).[12,13] Moreover, AmpC β-lactamase expression can increase in the nosocomial pathogens, triggered by exposure to antibiotics and β-lactamase inhibitors with the β-lactam function.[14,15] Therefore, AmpC β-lactamase is an important target for developing novel effective antibacterial therapies.

Several non-β-lactam inhibitors of class A and class C β-lactamases have already been reported in the literature, and intensive efforts have been made to optimize these molecules into new therapeutic agents. Boronic acid and phosphonate derivatives are transition state analogs that effectively inhibit class A and class C β-lactamases.[16−20] Non-β-lactam inhibitors are less likely to trigger β-lactam-induced resistance because their structurally dissimilar scaffolds can escape the recognition by β-lactamases, as well as sensor proteins responsible for inducing and mediating the expression of β-lactamases.[21] In addition, their activity is less affected by mutations on the porin

Received: February 5, 2012
Published: May 4, 2012

Chart 1. (A) Penicillin and cephalosporin hydrolysis by β-lactamases. (B) β-Lactamase inhibitors commonly used in the clinic. The β-lactam core is highlighted in red

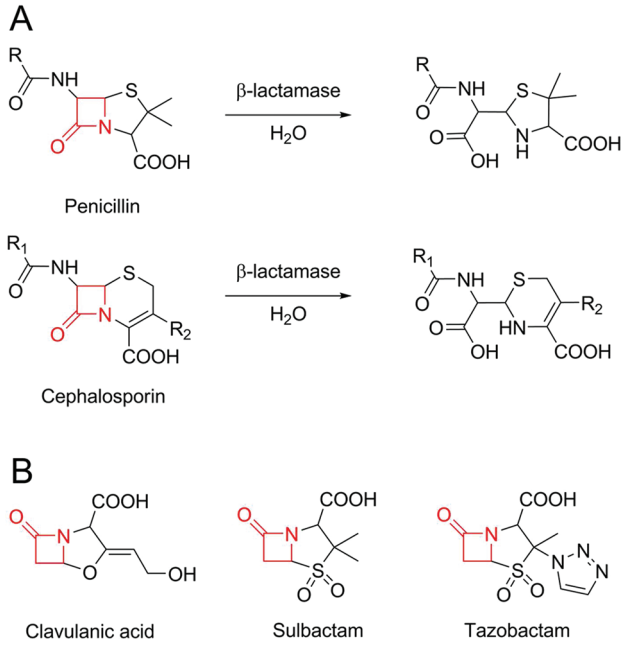

channel that prevent β-lactams from accessing their target. Unfortunately, both classes of compounds can form covalent adducts with serine proteases, thus reducing their selectivity against β-lactamases.[22] Taken together, it is highly desirable to develop new non-β-lactam inhibitors with a noncovalent mechanism of binding.

The increased availability of structural information on important pharmacological targets has greatly benefited the computer-aided drug design process. Recently, noncovalent AmpC β-lactamase inhibitors have been identified using structure-based[22−25] and ligand-based[26] virtual ligand screening (VLS) approaches. However, limitations of the structure-based docking approach have arisen from a low enrichment of true positives because a high percentage of the top-ranked compounds was experimentally identified as false positives.[22,27] As the active site of AmpC is highly exposed to the solvent, water-mediated interactions have been of particular importance for binding of noncovalent inhibitors because the water molecules could act as flexible connectors bridging the ligands to the enzyme. Another possible reason for the low enrichments in docking-based virtual screening is the induced-fit movements of highly flexible amino acid residues upon ligand binding.

To better understand the importance of ordered water molecules and active site plasticity on noncovalent ligand binding to AmpC, we performed molecular docking of known noncovalent inhibitors into the active site of multiple X-ray crystal structures with explicit water. The models were optimized and then structure-based virtual screening, using about 6 million compounds from commercially available

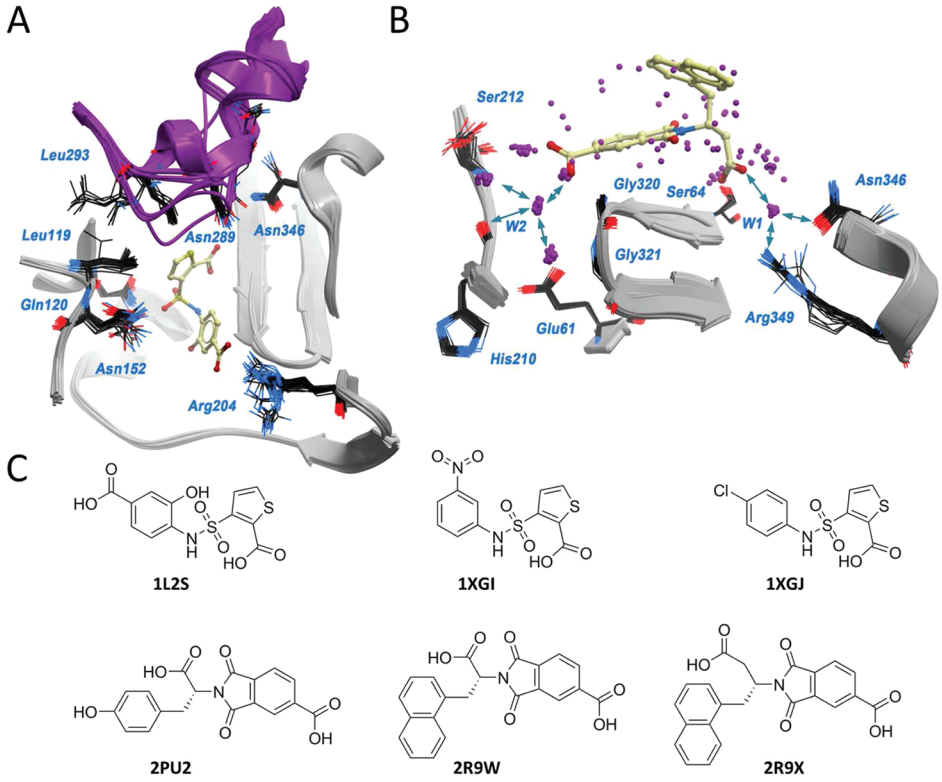

Figure 1. X-ray crystal structures of AmpC β-lactamase bound to noncovalent inhibitors were superimposed at the catalytic site. Panel A highlights the conformational plasticity of residues important for binding. A highly flexible helix formed by residues 279−293 is represented with a magenta ribbon. Water molecules from the multiple sites are represented in panel B with magenta spheres. Hydrogen bonds involving two clusters of conserved waters (W1 and W2) are shown with green arrows. Test set compounds for cross-dock validation of the AmpC active site models were extracted from the cocrystal structures and are shown in panel C. Small fragment-based inhibitors extracted for docking are shown in Chart S1 of the Supporting Information.

dx.doi.org/10.1021/ci300068m | J. Chem. Inf. Model. 2012, 52, 1367−1375

databases, was performed. Out of 61 chemically diverse compounds tested, seven new AmpC inhibitors were identified. These compounds might be used as new scaffolds for further development of antibacterial agents through a mechanism of AmpC-mediated β-lactamase inhibition.

MATERIALS AND METHODS

Protein Preparation. Nineteen X-ray crystal structures of AmpC β-lactamase bound to noncovalent inhibitors were retrieved from the Protein Data Bank (PDB entries 1KE4, 2BLS, 1L2S, 1XGI, 1XGJ, 2PU2, 2R9W, 2R9X, 2HDQ, 2HDR, 2HDS, 2HDU, 3GQZ, 3GR2, 3GRJ, 3GSG, 3GTC, 3GV9, and 3GVB)[20,22−25,28,29] and were prepared for docking using the protein conversion protocol implemented in ICM software.[30] Copies of the same protein within the asymmetric unit were treated independently as alternative conformational states of the AmpC active site (Figure 1A). Two clusters of ordered waters (W1 and W2) were identified after root-mean-square superimposition of the multiple AmpC binding pockets (Figure 1B). W1 is located at the catalytic site and mediates hydrogen bonds between most cocrystal ligands and the side chains of Asn346 and Arg349.[22,23,29] W2 is located outside of the catalytic pocket and is involved in a network of water-mediated hydrogen bonds between the series of phthalimide inhibitors and active site amino acids such as Glu61, His210, Ser212, Gly320, and Gly321.[29] Conserved water molecules were included or excluded from the docking runs using up to four hypothetical solvation states of each pocket conformation, i.e., including two water molecules, W1 only, W2 only, and no water molecules. For example, PDB entry 3GV9 was split into two water-free sites A and B (3GV9.a and 3GV9.b), four sites with one water molecule only (3GV9.aW1, 3GV9.bW1, 3GV9.aW2, and 3GV9.bW2), and two sites including both conserved water molecules (3GV9.aW1W2 and 3GV9.bW1W2). Nonconserved water molecules, phosphates ions, and other small molecules such as DMSO, PEG, and sugars were removed from the active site. As a result, 114 distinct models of AmpC were evaluated using molecular docking.

MMFF atom types were assigned to the protein atoms, cocrystal ligands, and water molecules.[31] Formal and partial charges were calculated at pH 7.4, and hydrogens were added and optimized to the best hydrogen bonding network. The three possible protonation states of histidines, as well as 180° flips of histidine, glutamine, and aspargine residues were attempted to optimize the hydrogen bonds using ICM software version 3.7-2a.[30] Moreover, the rotation of water molecules was optimized to the lowest energy conformation using Monte Carlo analysis. In a docking simulation, the ligand binding pocket was defined as a rectangular box large enough to accommodate all cocrystal ligands and extending additional 4 Å in any direction. Grid potential energy maps accounting for hydrophobic interactions, van der Waals potential, hydrogen bonds and electrostatic interactions were calculated for each pocket using a 0.5 Å grid spacing.

Ligand Preparation. For ligand binding mode prediction, the cocrystal ligands (Figure 1C and Chart S1) were extracted from the AmpC structures. The extracted ligands were converted into 1D using SMILES notation and then converted into 3D again and minimized using ICM software version 3.7−2a.[30] This procedure generated starting conformations for docking that are independent from the cocrystal geometries. For virtual ligand screening, about 6 million compounds from the Chembridge, Enamine, ChemDiv, NCI, and Interchim databases were downloaded using MolCart of ICM software version 3.7-2a[30] and were converted into 3D. Duplicate molecules were excluded. The compounds were filtered to remove molecules with known reactive groups and unfavorable absorption/permeation properties using ICM software version 3.7-2a.[30] The Lipinski rule of five was used to remove compounds with molecular weight above 500, calculated octanol−water partition coefficient above 5, more than 5 hydrogen bond donors and more than 10 hydrogen bond acceptors.[32] Compounds with polar surface area above 120 Å^2 were also excluded. To prevent chemical redundancy between known noncovalent AmpC inhibitors and compounds from the screening databases, binary fingerprints were calculated for all screening compounds and known noncovalent AmpC inhibitors selected from the directory of useful decoys (DUD) using ICM software version 3.7-2a.[30] The DUD is a benchmarking test set freely available on the Internet that provides active ligands and benchmarking decoys for 40 different targets (http://dud.docking.org/).[33] The Tanimoto coefficient, defined as $T = C/(A + B - C)$, where A is the number of nonzero bits for molecule A (screening compound), B is the number of nonzero bits for molecule B (known noncovalent AmpC inhibitor), and C is the number of nonzero bits common to A and B, was calculated for each pair of compounds using ICM software version 3.7-2a.[30] Compounds with Tanimoto distance (chemical dissimilarity) less than 0.3, defined as $1 - T$, were excluded. For the remaining molecules, stereoisomers were generated for racemic compounds, and protonation states were calculated at pH 7.4 using the automatic pK_a model implemented in ICM software version 3.7-2a.[30]

Pocket Refinement Protocol. Induced-fit movements upon binding of noncovalent AmpC inhibitors were simulated in PDB entries 1L2S, 1XGI, 1XGJ, 2PU2, 2R9W, and 2R9X using the ICM fully flexible docking algorithm.[34] For each pocket, residues with side chain heavy atoms within a 5 Å cutoff distance from the cocrystal ligand were allowed to randomly move using the ICM Biased Probability Monte Carlo algorithm, followed by a full local energy minimization.[35] Geometrically diverse low-energy conformations were saved and used for docking.

Benchmarking Protocol. The multiple conformations of the AmpC catalytic site derived from the X-ray crystal structures and induced-fit models, with and without conserved water molecules, were benchmarked for ligand binding mode prediction and virtual ligand screening. A test set combining 21 noncovalent AmpC inhibitors and 786 decoys was downloaded from DUD version 2 (http://dud.docking.org/).[33] Benchmarking decoys have similar molecular weight, number of hydrogen bonding groups, logP, and number of rotatable bonds compared to the active compounds, but their molecular topologies are different. The 3D geometries were optimized with ICM software version 3.7-2a[30], and the molecules were grouped into an annotated sdf file and docked against multiple representations of the AmpC catalytic site. Flexible ligand docking was performed with the ICM method that uses Monte Carlo to globally optimize a set of internal coordinates from the ligand in the space of grid potential maps calculated for the protein pocket.[36] The cocrystal ligands shown in Figure 1C and Chart S1 of the Supporting Information were also included in the file and docked. Three independent docking runs were performed with the maximal number of steps determined by an adaptive algorithm, according to the number of rotatable bonds

in the ligand multiplied by a thoroughness value set to 3. For each AmpC model, the top-scoring pose of each compound was selected for further analysis.

The predicted binding mode of cocrystal ligands was compared to the experimental coordinates using symmetry-corrected rmsd that accounts for topological symmetries of chemical groups (e.g., equivalent carbons in benzene rings or equivalent negatively charged carboxylic oxygens) and three-dimensional symmetries generated by rotation. Moreover, AmpC models were benchmarked for their ability to discriminate known AmpC inhibitors from benchmarking decoys using receiver operating characteristic (ROC) plots.[37] In a ROC curve, the true positive (TP) rate is plotted as a function of the false positive (FP) rate for all positions of the ranked score list. For an ideal model, all true positives are ranked higher than all top-scoring decoys. The resulting ROC plot passes through the upper left corner, and the area under the curve (AUC) is equal to 100. Normalized square root AUC (NSQ_AUC) was used in this study to combine the overall selectivity of linear ROC plots with early hit recognition properties, i.e., early ranking of active compounds in a large list of scores.[38] Briefly, a square root transformation was applied to the x-axis, and the maximal NSQ_AUC value was normalized to 100. According to this metric, random discrimination gives a NSQ_AUC value equal to zero.

Virtual Ligand Screening. Compounds of commercially available databases were docked against the final refined model of AmpC and ranked according to the predicted score. Top-scoring compounds with an ICM score below −30 and ligand binding efficiency below −1, defined as the ICM score divided by the number of heavy atoms, were clustered using binary fingerprints and the unweighted pair group method with arithmetic mean algorithm (UPGMA) implemented in ICM software version 3.7-2a.[30] Representative molecules with Tanimoto distance above 0.3 were selected from each cluster, and their binding modes were visually inspected. Sixty-one compounds predicted to mimic native contacts with AmpC β-lactamase catalytic site such as hydrogen bonds with Ser64, Asn152, or Ala318 were purchased and experimentally tested.

Biological Assay for AmpC Inhibition. The *Enterobacter cloacae* P99 AmpC β-lactamase gene was subcloned into a pRSETK vector that provided a stretch of a six histidine tag sequence upstream of the inserted gene. To achieve this, the AmpC gene was first amplified by a polymerase chain reaction (PCR) using plasmid pSG1113/M containing the AmpC β-lactamase gene as a template.[39] The PCR primers used were (forward) CGACTTCATATGACGCCAGTGTCAGAAAAA-CAGCTG and (reverse) CAGATTAAGCTTCGAATTCT-TACTGTAGCGCCTCGAGGATATG, which introduced the NdeI and *Hin*dIII restriction sites to the 5′ and 3′ ends of AmpC gene fragment, respectively. The PCR conditions were as follows: predenaturation at 94 °C for 5 min, 25 cycles of denaturation at 94 °C for 1 min, annealing at 44 °C for 1 min, elongation at 72 °C for 1 min, and the final step of further elongation at 72 °C for 7 min. The PCR product and pRSETK vector were then digested with restriction enzymes NdeI and *Hin*dIII respectively. The digested fragments of the vector and insert were gel-purified and then ligated. Calcium chloride-treated *E. coli* XL-1-Blue cells (sensitive to kanamycin) were transformed with the recombinant plasmids, and clones were selected on nutrient agar plates containing kanamycin (50 μg/mL). The identity of the clones was verified by DNA sequencing. The correct recombinant plasmid was transformed into *E. coli* BL21(DE3) for protein expression.

The AmpC β-lactamase protein was expressed in *E. coli* BL21(DE3) cells with a 6-histidine tag attached to its N-terminus under the control of a T7 promoter. The *E. coli* strain transformed with the β-lactamase gene was streaked on a nutrient agar plate containing 50 μg/mL kanamycin, and the agar plate was incubated at 37 °C overnight. The single colony from the agar plate was then inoculated into 5 mL of 2 × TY medium, which was then incubated at 37 °C with shaking at 250 rpm. After 16 h, the overnight culture was transferred into a fresh 2 × TY medium in a dilution ratio of 1:100 and grown at 37 °C with shaking at 250 rpm. When OD_{600} reached 0.8, protein expression was induced by adding 0.4 mM isopropyl β-D-1-thiogalactopyranoside (IPTG) to the bacterial cell culture. After induction, the culture was further incubated at 37 °C with shaking at 250 rpm for another 4 h, and then *E. coli* cells were harvested by centrifugation at 9000 rpm at 4 °C for 20 min. The cell pellet was resuspended in solubilization buffer (20 mM Tris, 50 mM NaCl, pH 8.0) and then lysed by lysozyme treatment and sonication. Afterward, the bacterial lysate was centrifuged at 10,000 rpm and 4 °C for 1 h. The supernatant containing 6-histidine tagged P99 AmpC β-lactamase was collected and loaded onto a nickel charged HiTrap chelating column pre-equilibrated with starting buffer (20 mM sodium phosphate buffer, 0.5 M NaCl, pH 7.4). The column was then washed with 6 column volumes of the starting buffer to remove the unbound proteins, and the histidine-tagged enzyme was eluted by a linear gradient of 0−0.2 M imidazole. Fractions containing AmpC β-lactamase were pooled, buffer-exchanged with 20 mM NH_4HCO_3 (pH 8.0) at 4 °C, lyophilized, and stored at −20 °C. A stock solution of P99 AmpC β-lactamase for the subsequent bioassay was prepared from the lyophilized powder.

Inhibitory activity of the test compounds against 0.1 μM P99 AmpC was conducted with 6.5 μM nitrocefin as the substrate by measuring changes in absorbance at 485 nm in 50 mM potassium phosphate buffer (pH 7.0) after 10 min of preincubation at room temperature.[40,41] Various concentrations of inhibitors were added in the presence of 0.01% freshly prepared Triton X-100 detergent.[42] Three independent assays were performed.

RESULTS AND DISCUSSION

Benchmarking Studies. The importance of protein plasticity in molecular recognition and structure-based drug design is well recognized, as is the relevance of target and software validation before undertaking the time- and cost-consuming screening of large compound databases.[43,44] As shown in Figure 1A, AmpC β-lactamase adopts alternative conformations to accommodate noncovalent ligands from different chemotypes such as small side chain rotations near the catalytic site (e.g., residues Gln120, Asn152, Arg204, and Asn348), as well as larger movements of a helix formed by residues 279−293.[25] Moreover, superimposition of multiple AmpC crystal structures revealed that the conserved water molecules involved in an extensive network of hydrogen bonds between the noncovalent inhibitors and the active site residues (Figure 1B). Previous studies suggested that inclusion of conserved water molecules in docking can improve the virtual ligand screening performance; however, this approach must be properly validated.[45] In this study, we investigated the role of

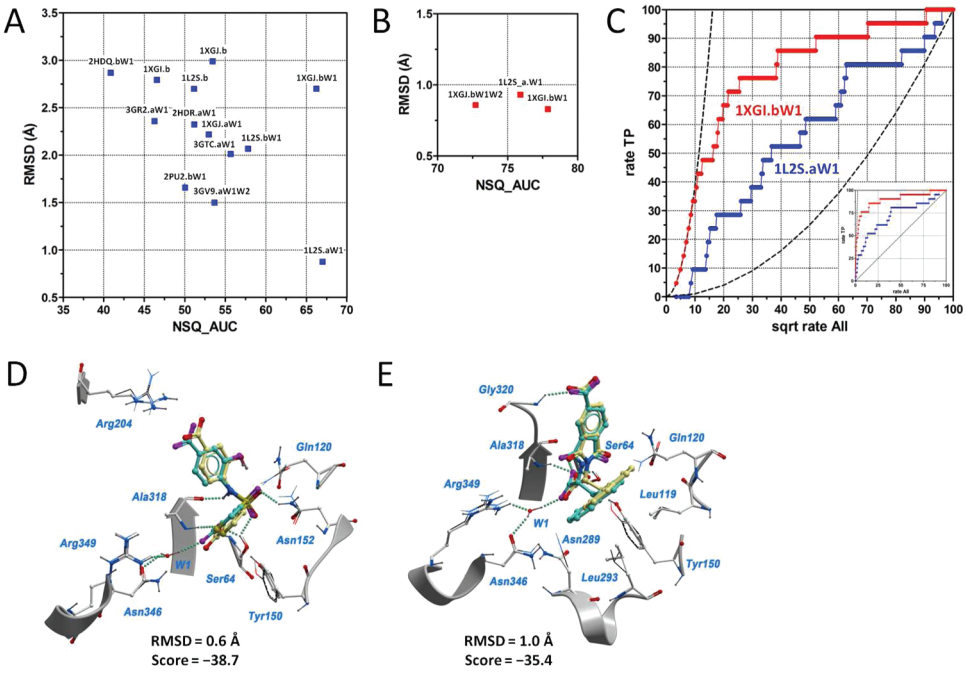

Figure 2. Ligand binding mode prediction and virtual ligand screening benchmark of the best-performing models before (A) and after (B) induced-fit analysis using fully flexible docking. AmpC cocrystal ligands were cross-docked, and the average rmsd was calculated. Normalized square root AUC values were derived from 21 noncovalent AmpC inhibitors and 786 benchmarking decoys available in the DUD test sets. Normalized square root ROC plots of the best-performing models, before and after refinement (1XGI.bW1, red; 1L2S.aW1, blue), are represented in panel C. Explicit water molecule W1 was used in both cases. The inset shows a linear version of the ROC plot. Panels D and E show the predicted binding modes of two representative noncovalent AmpC inhibitors. The predictions are represented with cyan carbons and magenta oxygens, whereas the cocrystal ligands are represented with yellow carbons and red oxygens. Hydrogen bonds are represented with spheres. The rmsd values and ICM scores are shown. Interacting residues are labeled and shown with a "ball and stick" model. For comparison, the initial unrefined conformations are shown with a wire model.

conserved water molecules and active site plasticity in noncovalent binding to AmpC β-lactamase.

Cross-docking simulations were performed on a number of known AmpC cocrystal ligands (Figure 1C) against their corresponding X-ray crystal structures.[20,22−25,28,29] Models with or without conserved water molecules (W1 and W2, Figure 1B) were generated as described in the Materials and Methods section. Moreover, binding site recognition for known AmpC inhibitors was benchmarked using the DUD test set combining 21 noncovalent binders with 786 decoys.[33] As shown in Figure 2A, inclusion of water molecule W1 was critically important for the accurate prediction of ligand binding modes and improvement of the VLS enrichments in comparison to the implicit treatment of solvation. Out of the 13 best models with average cross-docking rmsd below 3 Å and NSQ_AUC above 40, water molecule W1 was found in a total of 10 cases. On the contrary, water-free models 1XGI.b, 1L2S.b, and 1XGJ.b showed moderate VLS enrichments and average cross-docking rmsd above 2.5 Å. Although the water molecule W2 alone did not significantly improve the docking performance, W2 combined with W1 in model 3GV9.aW1W2 resulted in one of the best models with average rmsd = 1.5 Å in the cross-dock prediction and NSQ_AUC = 53.7 in the VLS study. Out of 114 nonrefined active site representations, 1L2s.aW1 was the best AmpC model with average cross-dock rmsd = 0.9 Å and NSQ_AUC = 67.0 (Figure 2A). Fragment-based inhibitors (Chart S1 of the Supporting Information)[25] were cross-docked into the multiple models of the AmpC active site with average rmsd predictions between 3.8 and 5.1 Å. Indeed, predicting fragment binding modes using molecular docking is a challenging issue due to the induced-fit movements. With analysis of several X-ray cocrystal structures of AmpC and fragments, we found that these molecules bound to different parts of the AmpC binding site. Some of these binding modes are associated with unique conformations of the highly flexible helix formed by residues 279−293 that cannot be reproduced in cross-docking experiments. As a result, fragments yield larger rmsd values than high molecular weight AmpC inhibitors.

Our results suggest that induced-fit analysis is important for molecular docking against AmpC β-lactamase. The models were refined using a Monte Carlo conformational search method to account for ligand binding site plasticity. Improvements in cross-docking accuracy and virtual ligand screening enrichments were found as compared to the unrefined models. As shown in Figure 2B, the best average rmsd predictions and virtual ligand screening enrichments were obtained with refined models from 1XGJ.bW1W2 (average rmsd = 0.9, NSQ_AUC = 72.7), 1L2S.aW1 (average rmsd = 0.9, NSQ_AUC = 75.9), and 1XGI.bW1 (average rmsd = 0.8, NSQ_AUC = 77.9). In particular, the refined model 1XGI.bW1 showed very good early enrichment for known annotated binders in the DUD test set, as opposed to nonrefined models (Figure 2C). Visual inspection of predicted protein−ligand complexes revealed that the small induced-fit movements of Arg204 and Asn152 can apparently enhance the strength of a salt bridge and the network of hydrogen bonds with known AmpC inhibitors (Figure 2D). Moreover, as shown in Figure 2E, small adjustments on the side chains of Gln120, Asn289, and Leu293 led to better shape complementarity between the AmpC active site and noncovalent inhibitors bearing bulky

dx.doi.org/10.1021/ci300068m | J. Chem. Inf. Model. 2012, 52, 1367−1375

Table 1. Inhibition of AmpC β-Lactamase Activity by Compounds 1−7 Selected from Structure-Based Virtual Ligand Screening with ICM

Compd	Structure	Vendor (code)	Tested concentration	% AmpC inhibition	IC_{50} (μM)[a]
1	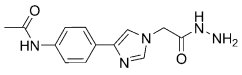	Chembridge (5367830)	384 μg/mL (1.4 mM)	65.7 %	ND[b]
2	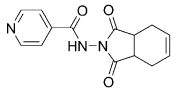	Chembridge (5907497)	384 μg/mL (1.4 mM)	49.3 %	ND[b]
3	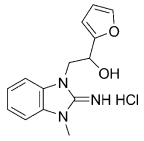	Chembridge (6043246)	384 μg/mL (1.3 mM)	61.7 %	ND[b]
4	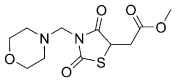	Chembridge (6246907)	384 μg/mL (1.3 mM)	71.9 %	ND[b]
5	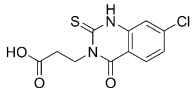	Enamine (T5361808)	384 μg/mL (1.3 mM)	84.8 %	ND[b]
6	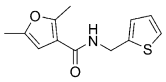	Chembridge (7947145)	192 μg/mL (0.82 mM)	82.3 %	351.3 ± 58.7
7	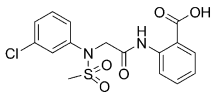	Chembridge (6463005)	384 μg/mL (1.0 mM)	73.9 %	784.8 ± 10.3

[a]Enzyme: P99 AmpC 0.1 μM; Substrate: nitrocefin 6.5 μM. [b]Not determined.

substituents. On the contrary, no significant improvement of ligand binding mode predictions for small fragment-based molecules was found after refinement. Predictions tended to mimic contacts with Ser64, Ala318, and W1, instead of exploring the alternative binding regions where some of the fragment bind. The ICM scores predicted for fragment-based inhibitors were less favorable than those predicted for larger AmpC inhibitors. However, the ligand binding efficacies, calculated as the ICM score divided by the number of heavy atoms, were more favorable for fragment-based inhibitors, suggesting that this measure might be useful for virtual ligand screening purposes.

On the basis of the above results, the best performing AmpC model refined from 1XGI.bW1 was selected for the subsequent virtual screening and prospective validation. The model incorporates one conserved water molecule and induced-fit side chain movements important for optimal binding of known molecules.

Virtual Ligand Screening. Commercially available compound databases were docked into the refined model of 1XGI.bW1. Prior to docking, the databases were filtered to remove duplicates, as well as compounds with poor predicted membrane permeability and known toxic motifs. After docking, compounds with an ICM score below −30 and ligand binding efficacy below −1 were retained and prioritized for experimental screening by taking into account the predicted binding mode, chemical diversity, molecular weight, and availability on the chemical vendor. Sixty-one chemically diverse molecules were then tested using the AmpC inhibition assay (Table 1 and Chart S2 of the Supporting Information).

Biological Evaluation. AmpC β-lactamase inhibition was initially tested by monitoring the hydrolytic activity of the enzyme against nitrocefin substrate, in the absence and in the presence of the test compounds. Nonionic Triton-X100 detergent was added to all experiments in order to suppress the formation of aggregates in solution and exclude aggregation-based promiscuous inhibitors.[42] Compounds **1**−**7** showed significant AmpC β-lactamase inhibition in the assay conditions used (Table 1). Activity drops in the range of 49.3−84.8% were achieved with concentrations ranging from 0.82 to 1.4 mM. Full dose−response curves were obtained for the most active compounds **6** and **7** with IC_{50} values of 351.3 ± 58.7 μM and 784 ± 10.3 μM, respectively (Figure S1 of the Supporting Information). The remaining 54 compounds selected from virtual ligand screening were inactive at the concentrations used (Chart S2 of the Supporting Information).

The moderate hit rate of 11% in this study might be related to the large, polar, and highly solvent-exposed binding pocket of AmpC. Indeed, catalytic site residues are highly flexible and are likely involved in transient and weak interactions with the noncovalent ligands. Despite these difficulties, we demonstrate that structure-based design of non-β-lactam AmpC inhibitors is an effective approach to identify new AmpC inhibitors. New chemotypes were identified, and compounds **5**−**7** were predicted to bind to the AmpC catalytic site and mimic known stabilizing contacts, such as hydrogen bonds with a conserved water molecule, Ser64 and Ala318, as well as hydrophobic interactions with Leu293, Tyr150, and Leu119 (Figure 3). It is noted that our model identifies inhibitors by noncovalent contacts, but compounds may also interact with

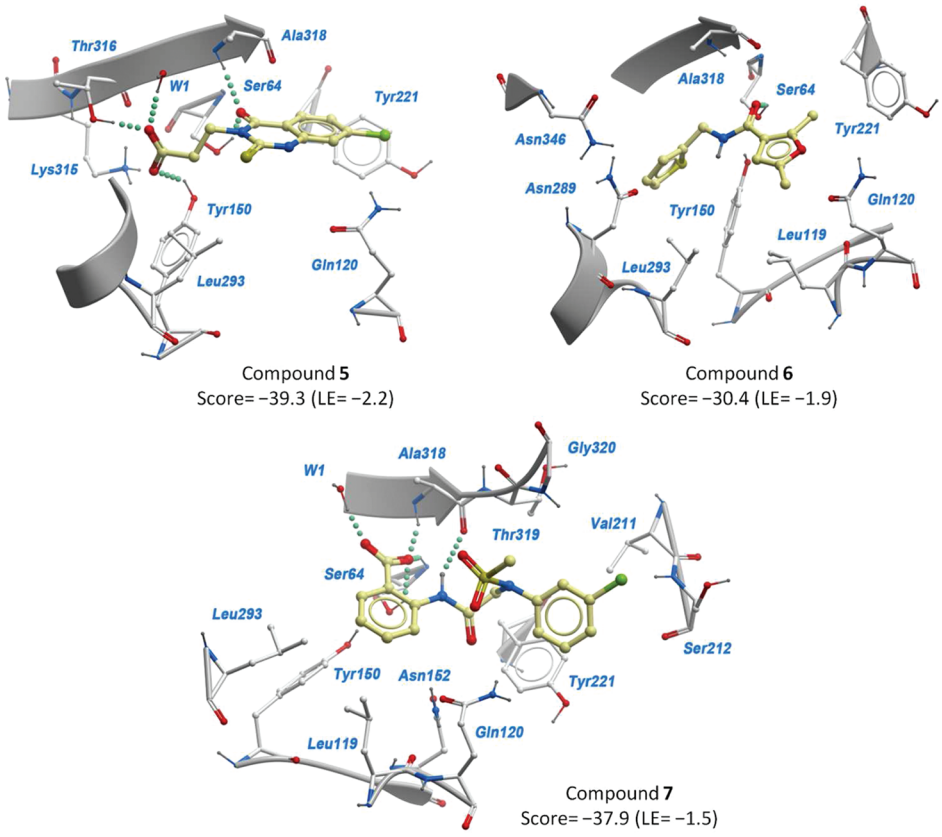

Figure 3. Predicted binding modes of new experimentally validated AmpC β-lactamase inhibitors **5**−**7**. The ligand binding site coordinates were obtained from a refined model derived from the PBD entry 1XGI (chain b) with one explicit water molecule. Interacting residues, ligands, and water molecule W1 are labeled and represented with a "ball and stick" model (protein carbon, white; small molecule carbon, light yellow; nitrogen, blue; oxygen, red; sulfur, dark yellow; chlorine, green; and polar hydrogens, gray). Hydrogen bonds are represented with spheres. Predicted ICM scores and ligand efficiencies (LE = ICM score/number of heavy atoms) are provided.

the residues in the active site through covalent and irreversible binding, which are not predicted by our model. Given the low molecular weight of compound **6** (MW = 235 Da) and the absence of a negatively charged group that is common to most of the noncovalent AmpC inhibitors known to date, this molecule can be considered a promising new AmpC β-lactamase inhibitor for the development of more potent compounds.

CONCLUSION

Given the continuous increase of β-lactamase-mediated resistance in bacteria, discovery of novel classes of non-β-lactam inhibitors is a promising approach to restore the activity of known antibiotics. In this work, we explored water-mediated interactions and active site plasticity to improve the cross-docking accuracy and VLS enrichment of models for the AmpC active site. Our benchmarking studies demonstrated the important role of explicit waters for binding of known noncovalent ligands. Two conserved water molecules have a bridging effect between the compounds and the enzyme; however, only one water molecule was critically important for accurate cross-docking predictions and improved discrimination between known actives and decoys. Moreover, induced-fit analysis using fully flexible docking suggests that small side chain readjustments of highly flexible AmpC binding site residues have a major impact for binding of noncovalent inhibitors. This finding has important implications for structure-based drug design using the ligand-guided approach. Currently, the number of potent noncovalent AmpC inhibitors from different chemotypes is very limited; however, as more and more compounds become available from experimental screening it will be possible to derive AmpC models with better predictive power, higher hit rates, and less false positives. Moreover, the confirmed inactive compounds reported in this study might be used to derive experimentally validated decoys and highly challenging test sets for docking, so as to refine the next generation of AmpC models.

Structure-based virtual screening of commercially available compounds identified seven previously unknown AmpC inhibitors. Compound **6** is a promising non-β-lactam AmpC inhibitor with low molecular weight and zero net charge. Given the novel molecular scaffolds and the encouraging computational and in vitro results, structure-based hit-to-lead optimization is currently underway in our laboratory.

ASSOCIATED CONTENT

Supporting Information

Known fragment-based inhibitors of AmpC β-lactamase used in cross-docking experiments, virtual ligand screening hit compounds confirmed inactive in the biological assay for AmpC inhibition, identification of chemical structure and purity of active compounds, and concentration−response plots of compounds **6** and **7**. This material is available free of charge via the Internet at http://pubs.acs.org.

AUTHOR INFORMATION

Corresponding Author

*Phone: +852 34003977. Fax: +852 23649932. E-mail: bckywong@polyu.edu.hk (K.-Y.W.). Phone: +1-858-822-3404. E-mail: ruben.ucsd.edu (R.A.).

Notes

The authors declare no competing financial interest.

ACKNOWLEDGMENTS

We acknowledge support from the Research Grants Council of Hong Kong (GRF PolyU 5023/08P), the Innovation and Technology Commission, and The Hong Kong Polytechnic University. M.A.C. Neves thanks Fundação para a Ciência e a Tecnologia (FCT), Portugal, for a Post Doctoral grant (SFRH/BPD/64216/2009).

REFERENCES

(1) Levy, S. B.; Marshall, B. Antibacterial resistance worldwide: Causes, challenges and responses. *Nat. Med.* **2004**, *10*, S122−S129.

(2) Neu, H. C. The crisis in antibiotic resistance. *Science* **1992**, *275*, 1064−1073.

(3) Barza, M.; Gorbach, S. L. The need to improve antimicrobial use in agriculture: Ecological and human health consequences. *Clin. Infect. Dis.* **2002**, *34*, S71−S144.

(4) Waxman, D. J.; Strominger, J. L. Penicillin-binding proteins and the mechanism of action of beta-lactam antibiotics. *Annu. Rev. Biochem.* **1983**, *52*, 825−869.

(5) Nikaido, H. Molecular basis of bacterial outer membrane permeability. *Microbiol. Mol. Biol. Rev.* **2003**, *67*, 593−656.

(6) Hancock, R. E. The bacterial outer membrane as a drug barrier. *Trends Microbiol.* **1997**, *5*, 37−42.

(7) Bennett, P. M.; Chopra, I. Molecular basis of beta-lactamase induction in bacteria. *Antimicrob. Agents Chemother.* **1993**, *37*, 153−158.

(8) Livermore, D. M. β-Lactamase-mediated resistance and opportunities for its control. *J. Antimicrob. Chemother.* **1998**, *41*, 25−41.

(9) Beceiro, A.; Bou, G. Class C β-lactamases: An increasing problem worldwide. *Rev. Med. Microbiol.* **2004**, *15*, 141−152.

(10) George, A. J. AmpC β-Lactamases. *Clin. Micorbiol. Rev.* **2009**, *22*, 161−182.

(11) Livermore, D. M.; Woodford, N. The β-lactamase threat in *Enterobacteriaceae*, *Pseudomonas* and *Acinetobacter*. *Trends Microbiol.* **2006**, *14*, 413−420.

(12) Bassetti, M.; Ginocchio, F.; Mikulska, M. New treatment options against gram-negative organisms. *Crit. Care* **2011**, *15*, 215−223.

(13) Page, M. G. β-Lactamase inhibitors. *Drug Resist. Updat.* **2000**, *3*, 109−125.

(14) Jacobs, C.; Huang, L. J.; Bartowsky, E.; Normark, S.; Park, J. T. Bacterial cell wall recycling provides cytosolic muropeptides as effectors for β-lactamase induction. *EMBO J.* **1994**, *13*, 4684−4694.

(15) Hanson, N. D.; Sanders, C. C. Regulation of inducible AmpC β-lactamase expression among *Enterobacteriaceae*. *Curr. Pharm. Des.* **1999**, *5*, 881−894.

(16) Beesley, T.; Gascoyne, N.; Knotthunziker, V.; Petursson, S.; Waley, S. G.; Jaurin, B.; Grundstrom, T. The inhibition of class C β-Lactamases by boronic acids. *Biochem. J.* **1983**, *209*, 229−233.

(17) Rahil, J.; Pratt, R. F. Phosphonate monoester inhibitors of class A β-lactamases. *Biochem. J.* **1991**, *275*, 793−795.

(18) Lobkovsky, E.; Billings, E. M.; Moews, P. C.; Rahil, J.; Pratt, R. F.; Knox, J. R. Crystallographic structure of a phosphonate derivative of the *Enterobacter cloacae* P99 cephalosporinase: mechanistic interpretation of a β-lactamase transition-state analog. *Biochemistry* **1994**, *33*, 6762−6772.

(19) Eidam, O.; Romagnoli, C.; Caselli, E.; Babaoglu, K.; Pohlhaus, D. T.; Karpiak, J.; Bonnet, R.; Shoichet, B. K.; Prati, F. Design, synthesis, crystal structures, and antimicrobial activity of sulfonamide boronic acids as β-lactamase inhibitors. *J. Med. Chem.* **2010**, *53*, 7852−7863.

(20) Powers, R. A.; Shoichet, B. K. Structure-based approach for binding site identification on AmpC β-lactamase. *J. Med. Chem.* **2002**, *45*, 3222−3234.

(21) Powers, R. A.; Blazquez, J.; Weston, G. S.; Morosini, M. I.; Baquero, F.; Shoichet, B. K. The complexed structure and antimicrobial activity of a non-β-lactam inhibitor of AmpC β-lactamase. *Protein Sci.* **1999**, *8*, 2330−2337.

(22) Powers, R. A.; Morandi, F.; Shoichet, B. K. Structure-based discovery of a novel, noncovalent inhibitor of AmpC β-lactamase. *Structure* **2002**, *10*, 1013−1023.

(23) Tondi, D.; Morandi, F.; Bonnet, R.; Costi, M. P.; Shoichet, B. K. Structure-based optimization of a non-β-lactam lead results in inhibitors that do not up-regulate β-lactamase expression in cell culture. *J. Am. Chem. Soc.* **2005**, *127*, 4632−4639.

(24) Babaoglu, K.; Shoichet, B. K. Deconstructing fragment-based inhibitor discovery. *Nat. Chem. Biol.* **2006**, *2*, 720−723.

(25) Teotico, D. G.; Babaoglu, K.; Rocklin, G. J.; Ferreira, R. S.; Giannetti, A. M.; Shoichet, B. K. Docking for fragment inhibitors of AmpC β-lactamase. *Proc. Natl. Acad. Sci. U.S.A.* **2009**, *106*, 7455−7460.

(26) Hsieh, J. H.; Wang, X. S.; Teotico, D.; Golbraikh, A.; Tropsha, A. Differentiation of AmpC beta-lactamase binders vs. decoys using classification kNN QSAR modeling and application of the QSAR classifier to virtual screening. *J. Comput. Aided Mol. Des.* **2008**, *22*, 593−609.

(27) Graves, A. P.; Brenk, R.; Shoichet, B. K. Docoys for docking. *J. Med. Chem.* **2005**, *48*, 3714−3728.

(28) Usher, K. C.; Blaszczak, L. C.; Weston, G. S.; Shoichet, B. K.; Remington, S. J. Three-dimensional structure of AmpC β-lactamase from *Escherichia coli* bound to a transition-state analogue: Possible implications for the oxyanion hypothesis and for inhibitor design. *Biochemistry* **1998**, *37*, 16082−16092.

(29) Babaoglu, K.; Simeonov, A.; Lrwin, J. J.; Nelson, M. E.; Feng, B.; Thomas, C. J.; Cancian, L.; Costi, M. P.; Maltby, D. A.; Jadhav, A.; Inglese, J.; Austin, C. P.; Shoichet, B. K. Comprehensive mechanistic analysis of hits from high-throughput and docking screens against β-lactamase. *J. Med. Chem.* **2008**, *51*, 2502−2511.

(30) *ICM*, version 3.7-2a; MolSoft LLC: San Diego, CA, 2010; http://www.molsoft.com/.

(31) Halgren, T. A. Merck molecular force field.1. Basis, form, scope, parameterization, and performance of MMFF94. *J. Comput. Chem.* **1996**, *17*, 490−519.

(32) Lipinski, C. A.; Lombardo, F.; Dominy, B. W.; Feeney, P. J. Experimental and computational approaches to estimate solubility and permeability in drug discovery and development settings. *Adv. Drug Delivery Rev.* **2001**, *46*, 3−26.

(33) Huang, N.; Shoichet, B. K.; Irwin, J. J. Benchmarking sets for molecular docking. *J. Med. Chem.* **2006**, *49*, 6789−6801.

(34) Totrov, M.; Abagyan, R. Flexible protein−ligand docking by global energy optimization in internal coordinates. *Proteins* **1997**, 215−220.

(35) Abagyan, R.; Totrov, M. Biased probability Monte Carlo conformational searches and electrostatic calculations for peptides and proteins. *J. Mol. Biol.* **1994**, *235*, 983−1002.

(36) Abagyan, R.; Totrov, M.; Kuznetsov, D. ICM−A new method for protein modeling and design: applications to docking and structure prediction from the distorted native conformation. *J. Comput. Chem.* **1994**, *15*, 488−506.

(37) Triballeau, N.; Acher, F.; Brabet, I.; Pin, J. P.; Bertrand, H. O. Virtual screening workflow development guided by the "receiver operating characteristic" curve approach. Application to high-throughput docking on metabotropic glutamate receptor subtype 4. *J. Med. Chem.* **2005**, *48*, 2534−2547.

(38) Katritch, V.; Rueda, M.; Lam, P. C. H.; Yeager, M.; Abagyan, R. GPCR 3D homology models for ligand screening: Lessons learned from blind predictions of adenosine A2a receptor complex. *Proteins* **2010**, *78*, 197−211.

(39) Tsang, M. W.; Leung, Y. C. Overexpression of the recombinant *Enterobacter cloacae* P99 AmpC β-lactamase and its mutants based on a φ105 prophage system in *Bacillus subtilis*. *Protein Expr. Purif.* **2007**, *55*, 75−83.
(40) O'Callaghan, C. H.; Morris, A.; Kirby, S. M.; Shingler, A. H. Novel method for detection of β-lactamases by using a chromogenic cephalosporin substrate. *Antimicrob. Agents Chemother.* **1972**, *1*, 283−288.
(41) Bush, K.; Macalintal, C.; Rasmussen, B. A.; Lee, V. J.; Yang, Y. Kinetic interactions of tazobactam with beta-lactamases from all major structural classes. *Antimicrob. Agents Chemother.* **1993**, *37*, 851−858.
(42) McGovern, S. L.; Caselli, E.; Grigorieff, N.; Shoichet, B. K. A common mechanism underlying promiscuous inhibitors from virtual and high-throughput screening. *J. Med. Chem.* **2002**, *45*, 1712−1722.
(43) Morra, G.; Genoni, A.; Neves, M. A. C.; Merz, K. M.; Colombo, G. Molecular recognition and drug-lead identification: What can molecular simulations tell us? *Curr. Med. Chem.* **2010**, *17*, 25−41.
(44) Kufareva, I.; Ilatovskiy, A. V.; Abagyan, R. Pocketome: An encyclopedia of small-molecule binding sites in 4D. *Nucleic Acids Res.* **2012**, *40*, D535−D540.
(45) Huang, N.; Shoichet, B. K. Exploiting ordered waters in molecular docking. *J. Med. Chem.* **2008**, *51*, 4862−4865.